Nonlinearity mitigation for high-speed optical OFDM transmitters using digital pre-distortion

Yuan Bao,[1] Zhaohui Li,[1,*] Jianping Li,[1] Xinhuan Feng,[1] Bai-ou Guan,[1] and Guifang Li[2]

[1] *Institute of Photonics Technology, Jinan University, Guangzhou, China*
[2] *CREOL, University of Central Florida, USA*
[*] *li_zhaohui@hotmail.com*

Abstract: Optical orthogonal frequency-division multiplexing (OOFDM) signal is sensitive to nonlinear distortions induced by optical modulators. We propose and experimentally demonstrate a digital pre-distortion (DPD) algorithm to linearize the optical modulators including electro-absorption modulated lasers (EML) and Mach-Zehnder modulators (MZM) used in high-speed OOFDM transmitters. By using an adaptive DPD algorithm with a learning structure, the inverse transfer function of a modulator, which is based on a polynomial model, has been obtained. In the experiment, the performance improvements with and without considering the memory effects of the DPD model are illustrated. The two typical kinds of high-speed OOFDM signals with a bit rate up to 30-Gb/s have been implemented experimentally. The results show that the nonlinear distortion induced by optical modulators can be compensated by using the DPD algorithm to substantially improve the optical modulation index.

©2013 Optical Society of America

OCIS codes: (060.0060) Fiber optics and optical communications; (230.4110) Modulators.

References and links

1. D. Z. Hsu, C. C. Wei, H. Y. Chen, J. Chen, M. C. Yuang, S. H. Lin, and W. Y. Li, "21 Gb/s after 100 km OFDM long-reach PON transmission using a cost-effective electro-absorption modulator," Opt. Express **18**(26), 27758–27763 (2010).
2. W. R. Peng, I. Morita, H. Takahashi, and T. Tsuritani, "Transmission of high-speed (>100-Gb/s) direct-detection optical OFDM superchannel," J. Lightwave Technol. **30**(12), 2025–2034 (2012).
3. Y. T. Moon, J. W. Jang, W. K. Choi, and Y. W. Choi, "Simultaneous noise and distortion reduction of a broadband optical feedforward transmitter for multi-service operation in radio-over-fiber systems," Opt. Express **15**(19), 12167–12173 (2007).
4. Y. Shen, B. Hraimel, X. Zhang, G. E. R. Cowan, K. Wu, and T. Liu, "A novel analog broadband RF predistortion circuit to linearize electro-absorption modulators in multiband OFDM radio-over-fiber systems," IEEE Trans. Microw. Theory Tech. **58**(11), 3327–3335 (2010).
5. B. Hraimel and X. Zhang, "A low cost broadband predistortion linearized single drive x-cut Mach-Zehnder modulator for radio-over-fiber systems," IEEE Photon. Technol. Lett. **24**(18), 1571–1573 (2012).
6. D. R. Morgan, Z. Ma, J. Kim, M. G. Zierdt, and J. Pastalan, "A generalized memory polynomial model for digital predistortion of RF power amplifiers," IEEE Trans. Signal Process. **54**(10), 3852–3860 (2006).
7. L. Ding, G. T. Zhou, D. R. Morgan, Z. Ma, J. S. Kenney, J. Kim, and C. R. Giardina, "A robust digital baseband predistorter constructed using memory polynomials," IEEE Trans. Commun. **52**(1), 159–165 (2004).
8. D. J. F. Barros and J. M. Kahn, "Optical modulator optimization for orthogonal frequency-division multiplexing," J. Lightwave Technol. **27**(13), 2370–2378 (2009).
9. Z. Liu, M. A. Violas, and N. B. Carvalho, "Digital predistortion for RSOAs as external modulators in radio over fiber systems," Opt. Express **19**(18), 17641–17646 (2011).
10. T. Alves, J. Morgado, and A. Cartaxo, "Linearity improvement of directly modulated PONs by digital pre-distortion of coexisting OFDM-based signals," in *Proceedings of Advanced Photonics Congress*, (Optical Society of America, 2012), paper AW4A.2.

1. Introduction

Optical orthogonal frequency-division multiplexing (OOFDM) has been considered as a promising candidate of future large-capacity optical networks [1, 2]. For short reach optical interconnection systems, optical access networks and metropolitan optical networks, OOFDM

#184086 - $15.00 USD Received 28 Dec 2012; revised 4 Mar 2013; accepted 4 Mar 2013; published 15 Mar 2013
(C) 2013 OSA

techniques also have obvious advantages compared with the conventional modulation format due to its performance and flexibilities.

Electro-absorption modulated lasers (EMLs) are attractive in next-generation short-reach OOFDM interconnection networks because they offer low-cost, easy integration, low driving voltage and power dissipation [1]. Meanwhile, the Mach-Zehnder modulator (MZM) is widely used in terabit long-haul OOFDM transmission system because it offers low chirp characteristic and superior performance [2]. However, the inherent nonlinear effects induced by optical modulators cause intermodulation distortion (IMD) in OOFDMs system and result in bit error rate (BER) performance degradation. Since it is complicated for the receiver to compensate for the modulator nonlinearities in combination with the channel distortion, linearization technique at the optical transmitter can be much more efficient.

Optical feed-forward compensation technique has been proposed to reduce the nonlinear distortion induced by uncooled distributed-feedback (DFB) laser diodes in radio-over-fiber (ROF) systems [3]. However, this linearization approach requires delay alignment of the error cancellation loop, which can be quite complicated. A broadband RF pre-distortion circuit (PDC) has been demonstrated for the linearization of an EML and a single drive x-cut MZM in ROF links [4, 5]. In addition, when used in high-speed optical transmission at >1Gb/s, the performance of the PDC needs to be evaluated again. Digital pre-distortion (DPD) technique was first proposed to compensate for the nonlinearities induced by the high power amplifier in wireless communication [6, 7]. Optical modulator optimization for OFDM transmitter is proposed to overcome the nonlinear distortion of MZM and increase the optical power efficiency [8]. However, this DPD algorithm only discusses the MZM and is not suitable for other optical modulators. DPD for 20Msymbol/s 64 quadrature amplitude modulation (QAM) ROF system based on a reflective semiconductor optical amplifier (RSOA) was demonstrated in [9]. Recently, OFDM-based (GbE, LTE, WiMAX and UWB) direct modulated passive optical network (PON) employing DPD algorithm to linearize the DML was also reported [10]. However, to the best of the authors' knowledge, the performance of polynomial-based DPD algorithm used in high-speed OOFDM transmitters has not been presented yet.

In this paper, DPD algorithm based on polynomials for both complex- and real-valued OFDM (CVOFDM and RVOFDM) signals are demonstrated. The bit rates of CVOFDM and RVOFDM signals are 30-Gb/s and 20-Gb/s respectively. The robustness of the DPD algorithm is verified since the nonlinear distortion induced by the EML and the MZM is successfully compensated. Performances of memory and memoryless DPD algorithm are also compared. In addition, dynamic AM/AM and AM/PM characteristics of the modulators in CVOFDM system without and with DPD algorithm are illustrated. Error vector magnitude (EVM) and constellations are measured at different modulation indices. Suppression of out-of-band spectral regrowth induced by nonlinear distortion is also demonstrated. The differences between nonlinear characteristics of intensity modulated MZM and EML are demonstrated and the effective region of DPD algorithm is discussed.

2. OOFDM transmitter and polynomial-based DPD algorithm

The OFDM signal generation and OOFDM transmitter with DPD algorithm is shown in Fig. 1, where CVOFDM and RVOFDM methods are employed respectively. They can be used alone or in combination depending on various applications. CVOFDM is for ROF system or single sideband (SSB) optical transmission and RVOFDM is widely used in intensity modulation direct detection (IMDD) systems, e.g. PONs. Both the CVOFDM and RVOFDM generators consist of serial-to-parallel conversion, QAM symbol mapping, inverse fast Fourier transform (IFFT), cyclic prefix (CP) insertion and parallel-to-serial conversion. The difference between them is that the symbol vector fed into IFFT block in the RVOFDM generator should have conjugate symmetry. Then a DPD algorithm calculates the pre-distorted output signal for nonlinearity compensation. Digital-to-analog converters (DACs) convert the digital series to analog waveforms and low pass filters (LPFs) are used to prevent aliasing. An electronic IQ-mixer is used to combine the real and imaginary parts of CVOFDM signal while up-conversion is not needed for RVOFDM signal. After amplified by

#184086 - $15.00 USD Received 28 Dec 2012; revised 4 Mar 2013; accepted 4 Mar 2013; published 15 Mar 2013
(C) 2013 OSA

an electronic driver, the OFDM signal drives the optical modulator and a bias-T may be needed to bias the signal at the operating point of optical modulator. If the transmitter is used in a wavelength-division-multiplexing (WDM) system, a multiplexer (MUX) will be used to combine all the optical signals from wavelength λ_1 to λ_N.

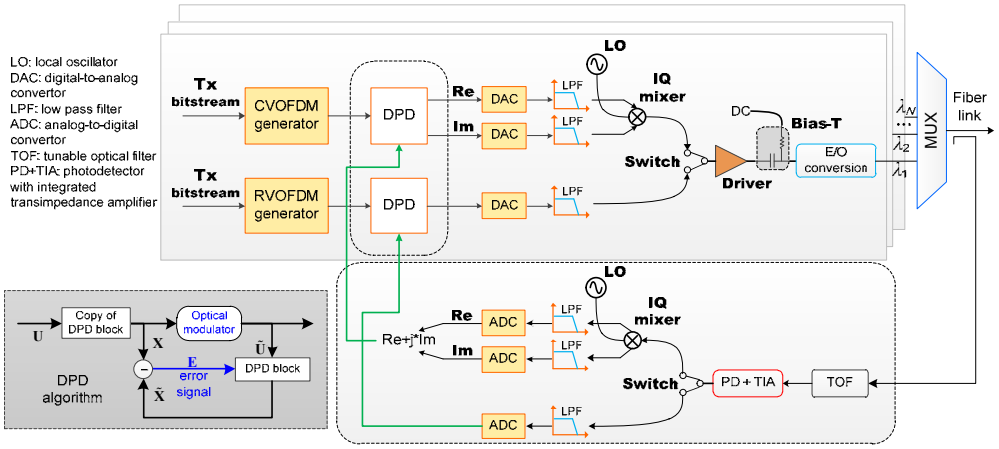

Fig. 1. The structure of the OOFDM transmitter with DPD algorithm (dashed line).

The OOFDM signal experiences nonlinear distortion in the optical modulator and the output is divided into two parts by an optical coupler or splitter, which establishes a feedback link after detection by a photo-detector (PD), while most of power will be fed into the fiber network for transmission. A tunable optical filter (TOF) is employed to select the channel which needs to be monitored if it is a WDM system. The feedback signal will pass through down-conversion circuits if the signal is up-converted. The baseband signal is filtered out by LPFs and then digitized by analog-to-digital convertors (ADCs).

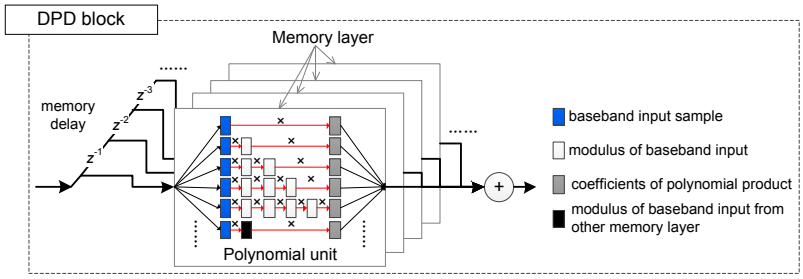

Fig. 2. The diagram of polynomial-based DPD block with memory effect.

In order to linearize the optical modulators, the adaptive DPD algorithm could be considered as a nonlinear equalizer in front of the optical modulator to pre-equalize the baseband signal by applying the inverse of modulator's transfer function. The feedback error is used to adjust the equalizer coefficients. As shown in the inset of Fig. 1, we utilize an adaptive DPD equalizer with an indirect training structure. The DPD block is placed first following the optical modulator and an identical copy is used to pre-distort the input. We assume that $\mathbf{U}$, $\mathbf{X}$, $\tilde{\mathbf{U}}$ and $\tilde{\mathbf{X}}$ are the signal vectors of original input, DPD output, ADC output and DPD output fed with ADC output, respectively. Let $\mathbf{E} = \mathbf{X} - \tilde{\mathbf{X}}$ be the error signal vector and solution to minimize the error $\| \mathbf{U} - \tilde{\mathbf{U}} \|^2$ is equivalent to minimize $\|\mathbf{E}\|^2$ [6]. Polynomials can be used to model the nonlinear transfer function of optical modulator. Accordingly, the inverse of optical modulator, can be written as $\tilde{\mathbf{U}} \cong f(\mathbf{X})$ and

#184086 - $15.00 USD Received 28 Dec 2012; revised 4 Mar 2013; accepted 4 Mar 2013; published 15 Mar 2013
(C) 2013 OSA

$\mathbf{X} = g(\mathbf{U}) \cong f^{-1}(\mathbf{U})$ respectively, where $f(\bullet)$ and $g(\bullet)$ are polynomial functions. If electrical-to-optical conversion suffers from memory effects due to the slow frequency response of the optical modulator, memory layers are needed for nonlinear compensation, as shown in Fig. 2. Thus, the calculation block of the DPD function $g(\bullet)$ following the optical modulator can be written as [6]

$$\begin{aligned}\tilde{x}(n) &= g(\tilde{u}(n)) \\ &= \underbrace{\sum_{m\in M_{sml}}\sum_{k\in K_{sml}} \tilde{u}(n-m)\,|\,\tilde{u}(n-m)\,|^{k}\, w_{mk}}_{\text{single memory layer}} + \underbrace{\sum_{m\in M_{cml}}\sum_{k\in K_{cml}}\sum_{l\in L_{cml}} \tilde{u}(n-m)\,|\,\tilde{u}(n-m-l)\,|^{k}\, w_{mkl}}_{\text{cross memory layer}} \\ &= \left[\tilde{u}(n)\right]_{\mathbf{polynomial}} \mathbf{w}.\end{aligned} \tag{1}$$

where $[\bullet]_{\mathbf{polynomial}}$ means packing all the polynomials of $\tilde{u}(n)$ in vector form and $\mathbf{w}$ which consists of w_{mk} and w_{mkl} is coefficients vector of $g(\bullet)$. M_{sml}, K_{sml} are the memory tap and nonlinear order index array in single memory layer and M_{cml}, K_{cml} are for cross memory layer, respectively. L_{cml} is the memory distances of cross memory terms. Thus, in vector form of $\tilde{\mathbf{U}}$ and $\tilde{\mathbf{X}}$, we have $\tilde{\mathbf{X}} = \tilde{\mathbf{U}}_{\mathbf{polynomial}}\mathbf{w}$ and the least square solution to minimize $\|\mathbf{E}\|^2$ is

$$\mathbf{w} = (\tilde{\mathbf{U}}_{\mathbf{polynomial}}{}^{H}\tilde{\mathbf{U}}_{\mathbf{polynomial}})^{-1}\tilde{\mathbf{U}}_{\mathbf{polynomial}}{}^{H}\mathbf{X}. \tag{2}$$

where $(\bullet)^{H}$ represents complex conjugate transpose. To lower the estimation error, the DPD coefficients can be trained adaptively with a step size of μ and the iteration function is written as follows [6]

$$\mathbf{w}_{p+1} = \mathbf{w}_{p} + \mu(\tilde{\mathbf{U}}_{\mathbf{polynomial}}{}^{H}\tilde{\mathbf{U}}_{\mathbf{polynomial}})^{-1}\tilde{\mathbf{U}}_{\mathbf{polynomial}}{}^{H}\mathbf{E}. \tag{3}$$

where $\mathbf{w}_0 = 0$ and $\mu < 1$. When Eq. (3) converges, the output of DPD block is as follows,

$$\mathbf{X} = \mathbf{U}_{\mathbf{polynomial}}\mathbf{w}. \tag{4}$$

Comment on the cost and complexity of DPD algorithm

The DPD algorithm needs to acquire the output signals for estimation of the polynomial coefficients and the transmitter must be accompanied by a high bandwidth receiver, including expensive high speed PD and ADC. The cost can be reduced in a WDM system, where the ADC is shared by all the channels, in which nonlinear estimation of each modulator works in different time period. To reduce the expense of the DPD algorithm in real time application, the sampled data can be stored and processed offline with accompanied processor. Since the characteristics of an optical modulator is slowly varying, the DPD algorithm can be run in open loop when Eq. (3) converges. Polynomial coefficients of each channel can be updated on an as needed basis.

3. Experimental setup and results

As shown in Fig. 3, we demonstrate two proof-of-concept experiments to verify the DPD algorithm, which is tested on CVOFDM and RVOFDM transmitters respectively. The input bit stream (PRBS length of 2^{15}-1) is parallelized and mapped into 16/32/64 QAM symbols. The subcarrier size is 512 and CP overhead is 1/32. The OFDM samples are generated offline in a MATLAB program and uploaded into an arbitrary waveform generator (Tektronix AWG 7122B) which is operated at 12-GS/s. The total bit rates of CVOFDM and RVOFDM signals are 30-Gb/s and 20-Gb/s, respectively. The bandwidth of LPF is 5.5-GHz and up-conversion frequency of CVOFDM signal is 9.3-GHz. The commercial EML and MZM are used as modulators under test in the experiments, respectively. The variable optical attenuator (VOA) is used to control the optical power for PD detection and the signal is then sampled by a real

#184086 - $15.00 USD Received 28 Dec 2012; revised 4 Mar 2013; accepted 4 Mar 2013; published 15 Mar 2013
(C) 2013 OSA

time oscilloscope (Tektronix DSA 72004B) at 50GS/s and 1M samples are recorded each time.

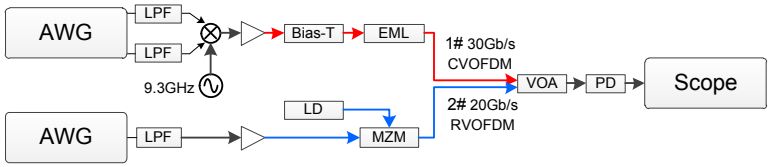

Fig. 3. Experimental setup of OOFDM transmitters with DPD algorithm. The EML and MZM are used to generate 30Gb/s CVOFDM signal and 20Gb/s RVOFDM signal, respectively.

The feedback samples are processed offline by a MATLAB program, including down-conversion, down sampling, DPD algorithm and OFDM demodulation. To reduce the DPD estimation error, transmitted samples $\mathbf{X}$ and corresponding output $\tilde{\mathbf{U}}$ need to be aligned before each estimation process. In addition, channel estimation of OFDM for clock recovery and carrier phase synchronization are also needed. However, in practical application, the OFDM demodulation step is not mandatory because the time delay of feedback link and carrier phase are fixed and can be measured for perfect alignment. Moreover, transmitting cyclic symbol block and using the average output for estimation will help to reduce the noise influence. The optical modulation index (OMI) and error vector magnitude (EVM) are used to evaluate the performance of the DPD algorithm. Here, $\mathrm{EVM} = \sqrt{\sum |(S_r - S_t)|^2 / \sum |S_t|^2}$, where S_r and S_t are respectively received and transmitted symbols; OMI = $(V_{in})_{RMS}/(V_{max}/2)$, where $(V_{in})_{RMS}$ is root mean square of the electric input to the optical modulators and V_{max} is maximum input voltage swing of EML, or switch voltage of MZM (V_π).

3.1 Experimental results of 30-Gb/s EML-based CVOFDM transmitter

First, a 30-Gb/s CVOFDM EML-based experiment is demonstrated with 16/32/64 QAM modulation formats, each having a different nonlinearity tolerance and bandwidth occupancy. The step size μ and memory effect are two key factors to improve the efficacy of the DPD algorithm. Here, the parameters of Eq. (3) chosen were $M_{sml} = \{0,1,2,3\}$, $K_{sml} = \{0,1, \ldots, 5\}$, $M_{cml} = \{0,1\}$, $K_{cml} = \{2,4\}$ and $L_{cml} = \{1,2,3\}$. If a particular polynomial coefficient is too small, this order and memory product can be ignored. Figure 4(a) shows measured EVM from transmitted 16QAM CVOFDM signal after several iterations under different values of μ. Obviously, Eq. (3) with larger μ converges fast but may be unstable and may even cause errors, while small μ reduces error, however converges slowly. Therefore, we chose $\mu = 0.7$ as a tradeoff between the stability and converging speed.

We also use the memoryless polynomial model of the DPD algorithm, which means that the memory terms in Eq. (1) are ignored, i.e., $M_{sml} = \{0\}$, $K_{sml} = \{0,1,\ldots,5\}$, M_{cml}, K_{cml} and L_{cml} are null. Then, the different performances with memory or memoryless DPD algorithms can be obtained. Figure 4(b) shows the measured EVMs of the transmitted 16/64QAM OOFDM

#184086 - $15.00 USD Received 28 Dec 2012; revised 4 Mar 2013; accepted 4 Mar 2013; published 15 Mar 2013
(C) 2013 OSA

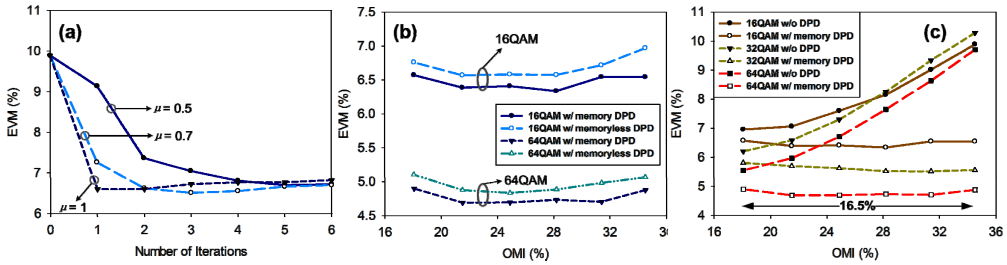

Fig. 4. Measured EVM results from the 30Gb/s CVOFDM system. (a) Transmitted EVM after iterations with different values of μ. (b) EVM of transmitted signal with memory or memoryless DPD algorithm. (c) EVM of transmitted signal with and without memory DPD algorithm.

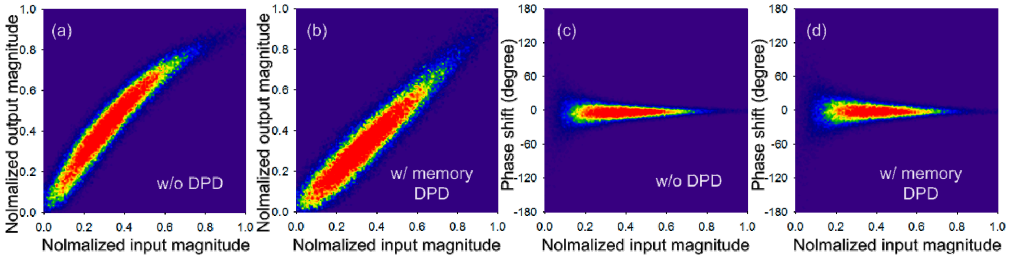

Fig. 5. AM/AM (a)(b) and AM/PM (c)(d) plots for received CVOFDM signal @OMI = 35% with and without memory DPD algorithm.

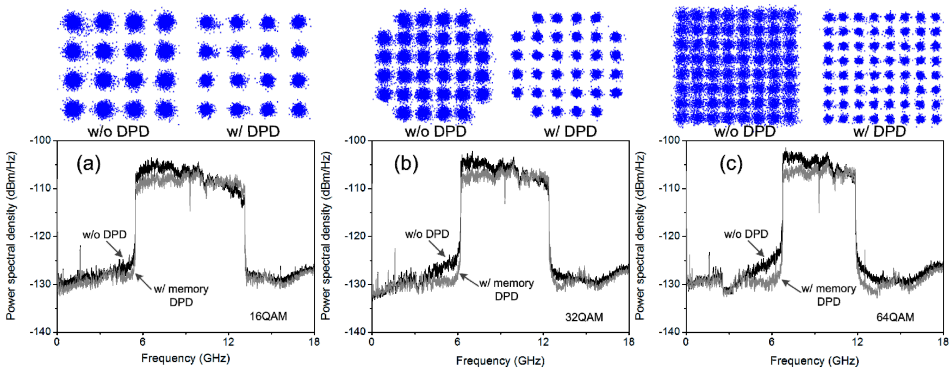

Fig. 6. Power spectral density and constellations of received CVOFDM signal @OMI = 35% with and without memory DPD algorithm. (a), (b) and (c) are 16QAM, 32QAM and 64QAM CVOFDM signals, respectively.

signal with the memoryless DPD and memory DPD algorithms. EVMs of 16/32/64QAM OOFDM signals vs. OMI with and without memory DPD algorithms are shown in Fig. 4(c). Here, the OMI range is selected from 18% to 34.5%. From Fig. 4(c), we can see that both the memoryless DPD and memory DPD algorithm can compensate for the nonlinearities of the EML. However, the performance of memory DPD algorithm is better than memoryless DPD. It can also be found that the memory DPD algorithm can improve the OMI over 16.5% to achieve the same EVM of 16/32/64QAM OOFDM signals.

By similarly illustrating the DPD linearization performance in the time domain, AM/AM and AM/PM plots are shown in Fig. 5. Among them, Figs. 5(a) and 5(b) show the AM/AM plots, while Figs. 5(c) and 5(d) show the AM/PM plots with and without memory DPD algorithm respectively. We can see the modulator suffer from magnitude nonlinearities as

#184086 - $15.00 USD Received 28 Dec 2012; revised 4 Mar 2013; accepted 4 Mar 2013; published 15 Mar 2013
(C) 2013 OSA

expected from Fig. 5(a). After using DPD algorithm, the nonlinearities can be largely compensated as shown in Fig. 5(b). Additionally, the power spectral density and constellations are also plotted in Fig. 6. We can see that the spectral growth out of band is suppressed (as shown in arrows) after using the DPD algorithm. Besides, since higher modulation formats suffer more severely from the nonlinear distortion, 64QAM OFDM signals are improved more than 16QAM.

3.2 Experimental results of 20-Gb/s MZM-based RVOFDM transmitter

The second experiment is demonstrated by using a 20-Gb/s MZM-based RVOFDM transmitter. The quadrature bias point of MZM is adopted for direct detection. The intensity transfer function of MZM modulator is shown in Fig. 7(a) and it can be divided into three regions: the linear region, the DPD effective region and the forbidden region. If the input voltage swing is small, the MZM modulator can be considered operating in linear region where the DPD algorithm is not required. When input voltage swing is increased but still smaller than V_{π}, there is a moderate nonlinear distortion and can be compensated by DPD algorithm. However, if the driving voltage is larger than V_{π}, the cosine transfer function leads to severe nonlinear distortion that the output peak signal is not clipped but reversed, which means that the signal falls into a forbidden region. In this case, the proposed DPD algorithm based on polynomials is not capable of modeling its inverse function, which is different from EML. The measured EVM with and without using the DPD algorithm are shown in Fig. 7(b) in which the different regions can be divided based on the improvement of the DPD algorithm. Noise influence can be found in the linear region (blue circles) when OMI is too small. Fortunately, the experimental result also shows that the OMI can be improved from about 9% to 16%.

To further verify the effectiveness of the DPD algorithm clearly, samples of input signal, output signal before and after compensation are plotted in Fig. 8. It can be seen that the DPD algorithm helps to regenerate the clipped peak signals and reduce the memory effect, as shown in Fig. 8.

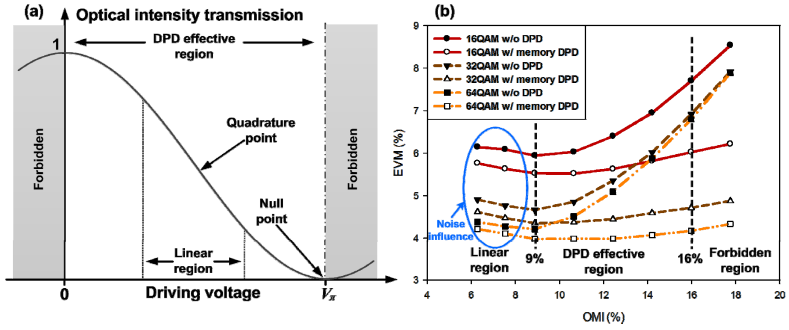

Fig. 7. (a) Linear region, DPD effective region and forbidden region of intensity modulation with MZM modulator. (b) Measured EVM results in the three regions with and without DPD algorithm.

#184086 - $15.00 USD Received 28 Dec 2012; revised 4 Mar 2013; accepted 4 Mar 2013; published 15 Mar 2013
(C) 2013 OSA

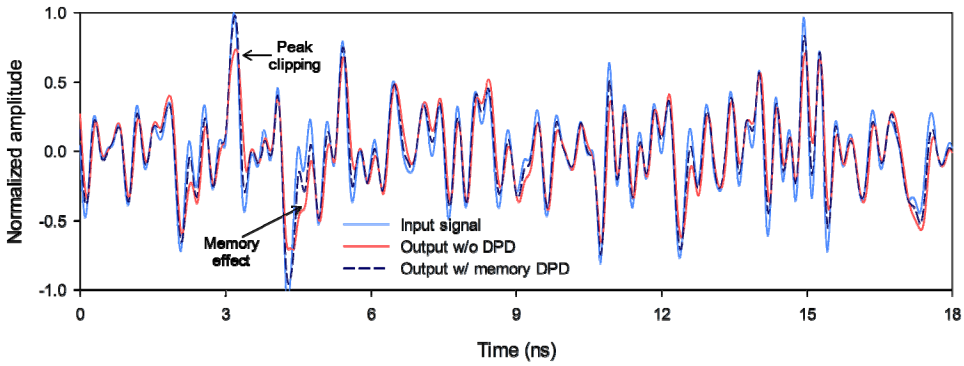

Fig. 8. Nonlinear distortion as peak clipping and memory effect induced by MZM modulator.

4. Conclusion

In this paper we have experimentally demonstrated a nonlinearity compensation technique for optical modulators based on the DPD algorithm. Commercial EMLs and MZMs are used under test and the experimental results show that OMI can be improved over 16.5% and 7% respectively by using the DPD algorithm. The DPD algorithm is optimized with a fast converging speed and low error. The experimental result also shows that the memory effect needs to be considered to achieve better performance. Forbidden region of intensity modulation by MZM should be avoided, since the nonlinearities cannot be fully compensated with the polynomial-based DPD algorithm in this case.

Acknowledgments

The authors would like to acknowledge the support from National Basic Research Programme of China (973) project (No.2012CB315603), National Natural Science Foundation of China (NSFC) under Grant No.61001101.

#184086 - $15.00 USD Received 28 Dec 2012; revised 4 Mar 2013; accepted 4 Mar 2013; published 15 Mar 2013
(C) 2013 OSA